# ORIGINAL PAPER

**Marcin A. Malik · Pawel J. Kulesza**
**Renata Wlodarczyk · Gunther Wittstock**
**Rüdiger Szargan · Henryk Bala · Zbigniew Galus**

# Formation of ultra-thin prussian blue layer on carbon steel that promotes adherence of hybrid polypyrrole based protective coating

**Abstract** Electrodeposition of well-adhering polypyrrole-based hybrid films containing hexacyanoferrate(II,III) anions from neutral solutions of pyrrole and potassium hexacyanoferrate(II) on medium carbon (0.48% C) steel has been described. The resulting polypyrrole coatings that are doped with hexacyanoferrate(II,III) anions show protective properties against pitting corrosion of carbon steel substrates in strongly acidic media containing chlorides (0.1 mol dm$^{-3}$ HCl + 0.4 mol dm$^{-3}$ NaCl). Polypyrrole acts as a stable host matrix for inorganic anions. The presence of negatively charged species (hexacyanoferrates) in the polymer backbone tends to block the access of pitting-causing anions (chlorides) to the surface of steel. The Fe(CN)$_6^{3-/4-}$ anions existing in the vicinity of steel substrate stabilizes its surface by forming an overcoating in the form of sparingly soluble metal hexacyanoferrate, mostly Prussian blue (PB), microstructures. It has been demonstrated that by applying cyclic voltammetry and X-ray photoelectron spectroscopy, the presence of traces of free cyanide anions promotes the formation of PB on carbon steel surface which results in increasing the adherence of polypyrrole-based films to the metallic substrate. Morphology of the protective composite films is also addressed.

Dedicated to Prof. G. Horanyi on the occasion of his 70th birthday

M. A. Malik · R. Wlodarczyk · H. Bala
Divison of Chemistry, Department of Materials
Processing Technology and Applied Physics,
Czestochowa University of Technology,
Al. Armii Krajowej 19, 42-201 Czestochowa,
Poland
E-mail: malik@mim.pcz.czest.pl
Fax: +48-34-3250705

P. J. Kulesza (✉) · Z. Galus
Department of Chemistry,
University of Warsaw,
Pasteura 1, 02-093 Warsaw,
Poland
E-mail: pkulesza@chem.uw.edu.pl
Fax: +48-22-8225996

G. Wittstock
Institute of Pure and Applied Chemistry and
Institute of Chemistry and Biology of Marine Environment,
Carl von Ossietzky University of Oldenburg,
26111 Oldenburg, Germany

R. Szargan
Departement of Chemistry, Wilhelm Ostwald
Institut of Physical and Theoretical Chemistry,
University of Leipzig, Linnéstr. 2,
04301 Leipzig, Germany

## Introduction

Thin films of polypyrrole doped with hexacyanoferrate(II,III) anions (PPy/hcnfe) have recently been considered for many practical applications in diverse areas such as biosensors [1–5], piezoelectric sensors [6], ion selective electrodes [7, 8], energy storage [9, 10] as well as for the fabrication of coatings for corrosion protection [11]. One of the most interesting features of this hybrid organic–inorganic material is its ability to undergo large charge accumulation due to the possibility of oxidation/reduction of both polypyrrole matrix and doping anions [8, 9, 12, 13]. Another important property of polypyrrole films containing hexacyanoferrate(II,III) anions, especially from the viewpoint of corrosion protection, is their cation-exchange character [7, 8]. Moreover, polypyrrole can be readily fabricated by electrodeposition. Finally,

the system shows stability and electroactivity in a fairly broad range of pH's.

In general, conducting polymer layers deposited on metallic substrates tend to stabilize a stationary potential within a passive range but they do not block the access of aggressive anions (e. g., chlorides) to their surfaces. In other words, they do not inhibit pitting corrosion of metals in a passive state [14–20]. There is a need of structural modification of conducting polymer-based films by changing their membrane properties, usually by incorporation of negatively charged species, for example, in the form of large immobile anions [8, 21, 22], into their structures. In our previous reports [11, 16, 17], we had described the protective properties of polypyrrole (PPy) and polyaniline films containing hexacyanoferrates(II,III) (hcnfe) deposited on stainless steel. Indeed, a strong suppression of pitting corrosion was observed even in the presence of high concentrations of chloride anions at low pH values because PPy/hcnfe composite films bearing negatively charged species are capable of blocking access of pitting-causing anions (chlorides) to the surface of a metal. In the case of PPy/hcnfe films prepared on stainless steel, a strong adherence to the metallic surface was induced by the addition of potassium cyanide at the 10 µmol dm$^{-3}$ concentration level. Thus, we also think that the presence of Fe(CN)$_6^{3-/4-}$ in the vicinity of steel substrate should lead to the stabilization of its surface by the precipitation of a thin overcoating film of a metal hexacyanoferrate, mostly Prussian blue (PB), i.e., iron hexacyanoferrate [22–29]. Consequently, the steel corrosion in acid media containing chlorides is largely suppressed.

This paper reports the successful preparation of robust, dense and well-adhering PPy-based structures on carbon steels in the presence of hexacyanoferrate anions. The concept of the formation of a thin PB interlayer on a steel substrate is verified by voltammetric and X-ray photoelectron spectroscopy (XPS) measurements. Moreover, the enormous improvement of the PPy/hcnfe adherence to the steel substrate by the presence of very low concentrations of cyanide ions in the modification solution has been elucidated.

## Experimental

The constructional carbon steel consists of the following components: 0.48% C, 0.56% Mn, 0.20% Si, <0.040% P, <0.040% S, <0.30% Cr, 0.30% Ni and <0.10% Mo, and <0.30% Cu was used as a working electrode. Before measurements, the electrode was activated by polishing on a waterproof emery paper up to 2,500 grade, then it was sonicated and, subsequently, washed with water. Saturated (KCl) calomel electrode (SCE) served as the reference electrode. The counter electrode was the Pt gauze.

The composite polymer films were electrodeposited from the solution of 0.75 mol dm$^{-3}$ pyrrole (monomer) + 0.1 mol dm$^{-3}$ K$_4$[Fe(CN)$_6$] + 10 µmol dm$^{-3}$ KCN. The deposition process was achieved galvanostatically (current density 0.02 A cm$^{-2}$) while the electrode (steel) potential was monitored simultaneously. Potentiodynamic (log current–potential) curves were recorded at 2 mV s$^{-1}$ scan rate. To evaluate the protective properties of composite films, chronoamperometric (current–time) curves were recorded at a constant potential of 0.5 V versus SCE (arbitrarily chosen from the potentiodynamic data characteristics of the steel in 0.1 M HCl + 0.4 M NaCl, usually as a potential at which the substrate undergoes rapid local dissolution).

All the chemicals were reagent grade and were used as received without further purification. Distilled and subsequently deionized water was used to prepare test solutions.

A multifunctional analyzer Model CHI660 (CH Instruments, Austin, TX, USA) was employed to perform electrochemical measurements. The film thickness was determined by profilometry (profilometer Form Talysurf 2, Taylor Hobson Ltd., UK). Scanning electron microscopy (SEM) images were obtained using JOEL Model JSM-5400 operating at 30-kV accelerating voltage. High-resolution photoelectron spectra were recorded using an ESCALAB 22i XL (VG, East Grinstead, West Sussex, UK) spectrometer, located at University of Leipzig, Germany. The 180° half sphere analyzer and monochromatized Al–K$\alpha$ X-ray excitation (Al anode, 12 kV, 20 mA, h$\nu$ = 1486.6 eV) were applied. The instrument was operated with a magnetic lens in the "large area XL-mode" with a pass energy of 10 eV. The line width of the Ag 5d$_{5/2}$ line used to calibrate the instrument is 0.5 eV, with 400 kcounts s$^{-1}$ under these circumstances. The binding energy of the Au 4f$_{7/2}$ line, used for the instrument calibration as well, was equal to 84.0 eV. Survey and detailed photoelectron spectra were recorded with 50 eV and 10 eV pass energies, respectively. Binding energies are given relative to the binding energy of C1s peak, $E_b$ = 284.6 eV (originating from carbon in adventitious hydrocarbons coming from diffusion pumps). The vacuum in the analyzing chamber was below 5×10$^{-9}$ mbar. An Ar$^+$ ion gun was used for a surface etching during depth profiling (1 min ion etching resulted in ca. 1 nm depth). Other experimental details are reported elsewhere [30].

## Results and discussion

Deposition of PPy/hcnfe films

Hybrid PPy/hcnfe films were electrodeposited galvanostatically from the solution described in the "Experimental section" following application of a constant current density of 0.02 A cm$^{-2}$ for 300 s or 900 s. Figure 1 illustrates a typical chronopotentiometric curve recorded during the galvanostatic electrodeposition of polypyrrole–hexacyanoferrate (PPy/hcnfe) composite film. It is noteworthy that, in the initial stage of electrodeposition, the system potential increased up to ca.
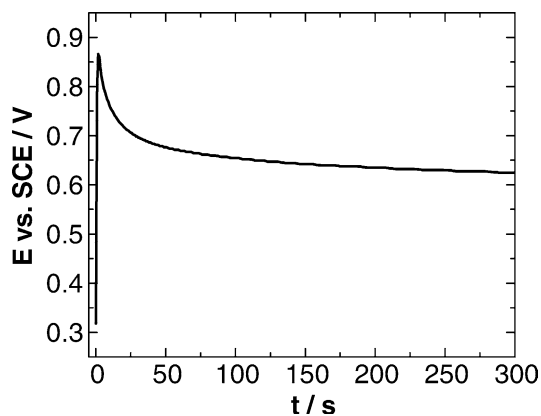
**Fig. 1** Dependence of electrode potential on time for the galvanostatic electrodeposition (on carbon steel) of the polypyrrole-based coating containing hexacyanoferrates. Current density 0.02 A cm$^{-2}$. Modification solution 0.75 mol dm$^{-3}$ pyrrole + 0.1 mol dm$^{-3}$ K$_4$[Fe(CN)$_6$] + 10 $\mu$mol dm$^{-3}$ KCN



**Fig. 2** The cross-sectional SEM view of the composite polypyrrole layer electrodeposited for 900 s from the solution of 0.75 mol dm$^{-3}$ pyrrole + 0.1 mol dm$^{-3}$ K$_4$[Fe(CN)$_6$] + 10 $\mu$mol dm$^{-3}$ KCN at the constant current density of 0.02 A cm$^{-2}$ (Magnification 1,000×)

0.85 V as a result of the initially occurring oxidation processes involving pyrrole monomer and hexacyanoferrate(II) ions. After approximately 100 s, the potential somewhat lowered and, during prolonged time of eletrodeposition, it reached the steady-state value of about 0.60 V. This result implies the completeness of polymerization, and it is consistent with the formation of PPy in its partially oxidized form that bears a positive (membrane) charge. Consequently, hexacyanoferrate anions must have been electrostatically attracted and trapped within the conducting polymer film. It can be expected that, during electrodeposition of PPy/hcnfe film on carbon steel, hexacyanoferrate anions would interact with iron(II,III) to form sparingly soluble metal hexacyanoferrate, predominantly a thin PB layer adhering to the steel surface.

The resulting films adhered very well to carbon steel substrates, what was verified by applying a simple test with Scotch tape. The strong adherence of PPy/hcnfe coatings was also proved by the SEM examination of the carbon steel/polymer coating interface. The cross-sectional view of the carbon steel sample covered with PPy/hcnfe film (electrodeposited for 900 s) is shown in Fig. 2. It is clearly seen from the data of Fig. 2 that PPy/hcnfe film uniformly covered the steel substrate. The thickness of the film, when measured from the cross-sectional image, was ca. 35 $\mu$m, and it corresponded well with the measurement obtained from profilometry, 36 $\mu$m. Application of shorter electrodeposition time, i.e., 300 s, produced the film of thickness equal to 9 $\mu$m.

In order to elucidate the influence of the electrodeposition time on the morphology of composite films on carbon steel, we recorded SEM measurements. It is apparent from the SEM data (Fig. 3) that the polypyrrole-based films containing hexacyanoferrates are uniform but they exhibit globular structure. The size of globules formed is independent on the electrodeposition time, at least within electrodeposition time intervals
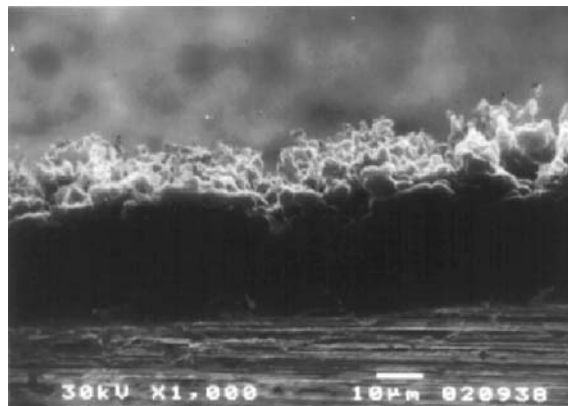
considered here. The globules characteristic of the PPy/hcnfe films are on the level of 5 $\mu$m. Globular aggregates are pillared, and they form fairly dense structures.

Formation of PB on carbon steel surface

Our previous results indicated that an addition of trace amounts of cyanide anions to the modification solution improves the adhesion properties of the composite film, and mostly facilitates formation of the interfacial PB film [11]. In order to verify this hypothesis, detailed voltammetric and surface analyses were done for steel samples subjected to the electrolytes analogous to that had been used for polymer electrodeposition (but in the absence of pyrrole monomer), namely 0.1 mol dm$^{-3}$ K$_4$Fe(CN)$_6$ with and without additions of free cyanide anions (at the concentration level of 10 $\mu$mol dm$^{-3}$). Samples were conditioned for 450 s at the constant potential, 0.6 V versus SCE, that is close to the potential established during galvanostatic deposition of PPy/hcnfe films (Fig. 1). Cyclic voltammograms recorded in 0.5 mol dm$^{-3}$ KNO$_3$ for carbon steel samples (pretreated as described above) are shown in Fig. 4. For the sake of comparison, the voltammogram of bare steel sample is also shown. Potassium nitrate was chosen as the supporting electrolyte because PB is electroactive in the presence of K$^+$ cations [22–28], i.e., undergo redox reactions at potentials: ca. 0.2 V [characteristic of the oxidation/reduction of nitrogen coordinated high spin Fe(II,III) ions] and ca. 0.85 V [characteristic of the oxidation/reduction of iron ions in Fe(CN)$_6^{4-/3-}$ groups]. For the so called "soluble" (i.e., containing potassium ions) form of PB, KFe$^{III}$[Fe$^{II}$(CN)$_6$], the redox reactions are described using the following equations [22–28]:

$$K_2Fe^{II}[Fe^{II}(CN)_6] \Leftrightarrow KFe^{III}[Fe(CN)_6] + K^+ + e^-$$
at 0.2 V vs. SCE (1)

$$KFe^{III}[Fe^{II}(CN)_6] \Leftrightarrow Fe^{III}[Fe^{III}(CN)_6] + K^+ + e^- \qquad (2)$$
at 0.85 V vs. SCE

In the case of the bare carbon steel sample, only one oxidation peak (marked with an asterisk in Fig. 4a) is visible in the first scan starting from −0.2 V which disappears in next voltammetric cycles (not shown in Fig. 4). This peak is related to the oxidation of iron and the formation of a passive layer. When the carbon steel sample has been conditioned in 0.1 mol dm$^{-3}$ K$_4$Fe(CN)$_6$ solution and then transferred to 0.5 mol dm$^{-3}$ KNO$_3$ supporting electrolyte, the oxidation peak related to the steel passivation has become much lower (note different scales in Fig. 4) than for the bare steel sample. The result is consistent with the view that, during the conditioning in K$_4$Fe(CN)$_6$, a quite stable passive layer is formed on carbon steel. More important is the appearance of the voltammetric peaks at ca. 0.2 V and 0.85 V (marked with arrows in Fig. 4b) although they are poorly defined. This observation indicates the existence of traces of PB on the steel surface. Judging from the charge (estimated from the voltammetric peak at 0.2 V) consumed for the PB reduction, $Q = 51$ μC cm$^{-2}$, the PB surface coverage ($\Gamma$) is on the order of 0.53 nmol cm$^{-2}$. Knowing that the unit cell parameter ($a$) of PB is equal to 1.01 nm [31], the thickness ($l$) of the layer could be calculated according to the following equation [32]:

$$l = \frac{\Gamma a^3 N_A}{4} \qquad (3)$$

where $N_A$ stands for Avogadro number. In the case of the steel pretreated in 0.1 mol dm$^{-3}$ K$_4$Fe(CN)$_6$, the estimated PB thickness was equal to 0.8 nm, what suggested that the surface was not completely covered with PB or, in other words, the coverage was less than one monolayer.

In the case of the steel sample pretreated in the 0.1 mol dm$^{-3}$ solution of K$_4$Fe(CN)$_6$ containing 10 μmol dm$^{-3}$ KCN, the voltammetric response is dominated by well defined peaks coming from redox

reactions (Eqs. 1, 2) of iron(III) hexacyanoferrate(II), as shown in Fig. 4c. It should be noted that the substrate oxidation peak is even lower than peaks related to redox reactions of PB. The PB thickness estimated from the determination of charge, $Q = 140\ \mu C\ cm^{-2}$, consumed during PB reduction at the potential close to 0.2 V is equal to 2.2 nm. This value corresponds to the surface coverage by approximately two PB monolayers. Thus, we can conclude that the presence of free cyanide anions in the solution of potassium hexacyanoferrate(II) promotes the formation of PB on the carbon steel surface during conditioning at the potential of 0.6 V.

To evaluate the state of steel surface, following pretreatments in the presence and absence of cyanide anions, XPS measurements have been recorded. The XPS survey spectra for samples pretreated in the presence and absence of KCN, are shown in Fig 5. Differences in obtained spectra are clearly visible in binding energy regions, characteristics for potassium 2p, nitrogen 1s, carbon 1s and oxygen 1s peaks. In the case of the sample subjected to $K_4Fe(CN)_6$ and KCN solutions, the potassium content as well as the nitrogen and carbon contents on the surface were much higher than on the sample pretreated in the KCN-free $K_4Fe(CN)_6$ solution. The existence of potassium, nitrogen and carbon on the surface can be explained by assuming that a thin layer of PB ($KFe[Fe(CN)_6]$) exists on the steel surface subjected to the $K_4Fe(CN)_6$ solution containing potassium cyanide. On the contrary, the oxygen 1s peak is much lower in the case of the sample exposed to $CN^-$ containing solution when compared to the sample pretreated with $CN^-$-free solution.

The detailed $Fe2p_{3/2}$, O1s, N1s and K2p spectra recorded for samples exposed to 0.1 mol $dm^{-3}$ $K_4Fe(CN)_6$ (at 0.6 V) in the presence and absence of $CN^-$ ions are shown in Fig. 6. The C1s spectrum consisted of only one peak with the maximum at binding energy, $E_b = 284.6$ eV, that is equivalent to the position of hydrocarbons C1s signal coming from ubiquitous
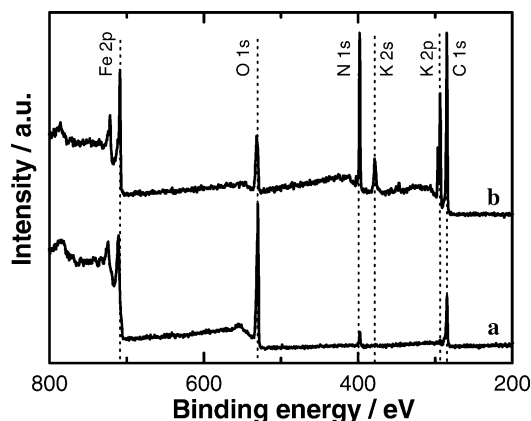
contaminations (mostly from diffusion pumps). Consequently, the C1s spectrum is not considered since there is no possibility to distinguish between the carbons coming from PB and adventitious carbon. The existence of adventitious carbon is also evident from the comparison of the surface concentrations of nitrogen and carbon (see further results concerning depth profiling). A much higher content of carbon in comparison to nitrogen has been found in both samples although the C:N ratio should be 1:1 in PB. The same C1s peak position for PB XPS spectrum is reported in literature [29]. The main differences between carbon steel samples pretreated in cyanide-free and cyanide containing environments are manifested in the spectra of $Fe2p_{3/2}$ (Fig. 6a, e) and O1s (Fig. 6b, f). For the sample exposed to $K_4Fe(CN)_6$ + KCN solution, the most intense peak on the $Fe2p_{3/2}$ spectrum is located at $E_b = 708.4$ eV, and two much smaller peaks appear at binding energies, 709.5 eV and 711.7 eV, respectively. The main peak presumably comes from the iron(II) ions coordinated by carbon atoms in $-Fe^{II}(CN)_6$ groups in PB. This result would be consistent with literature data, namely with the value of 708.8 eV obtained for PB deposited on polypyrrole film and conditioned at 0.7 V versus SCE in $K^+$ containing electrolyte [33, 34]. Moreover, the $Fe2p_{3/2}$ binding energy of 708.4 eV for $K_4Fe(CN)_6$ [35] and $E_b \approx 709$ eV for $Fe2p_{3/2}$ signal of Everitt's salt, $K_2Fe^{II}[Fe^{II}(CN)_6]$, i.e., for the reduced form of PB [29], have been reported. It is noteworthy that, for cobalt and nickel hexacyanoferrates(II), single $Fe2p_{3/2}$ peaks of similar shape to the peak denoted as $Fe(CN)_6^{4-}$ in Fig. 6a, were observed for $-Fe^{II}(CN)_6$ groups at the binding energy 708.0 eV [30]. The above discussion of the binding energy of the main peak of $Fe2p_{3/2}$ (for the sample pretreated in $K_4Fe(CN)_6$ + KCN solution) allows us to conclude that it originates from iron(II) ions in $-Fe^{II}(CN)_6$ groups from PB existing on the carbon steel surface. An explanation of the exact origin of two smaller peaks (Fig. 6a) is much more complicated because they might come either from nitrogen-coordinated iron(III) ions in PB or from iron(II,III) oxides/hydroxides forming passive layer on the carbon steel surface. The binding energy, 710 eV, was reported for Fe(III) ions in PB [33, 34]. This $E_b$ value is close to the maximum of the peak a in Fig. 6a ($E_b = 709.5$ eV). On the other hand, the binding energies for iron(II) ions in passive films on metallic iron and steels are in the range 709–710 eV [35–37]. Thus, it is likely that the peak at $E_b = 709.5$ eV reflects superposition of signals from Fe(III) ions from PB and Fe(II) ions originating from iron(II) oxides/hydroxides constituting the passive layer. Since Fe(III) ions also exist in a form of oxides/hydroxides in the passive layer, and the reported binding energies ($Fe2p_{3/2}$) for these ions are in the range from 710.5 eV to 711.5 eV [35–38], it is likely that the peak b in Fig. 6a (with the maximum at 711.6 eV) originates from Fe(III) ions in the oxide/hydroxide passive film. The $Fe2p_{3/2}$ signal recorded from the carbon steel sample pretreated in cyanide-free $K_4Fe(CN)_6$ solution



**Fig. 5** XPS survey spectra recorded for steel samples exposed for 450 s to **a** 0.1 mol $dm^{-3}$ $K_4Fe(CN)_6$, and **b** 0.1 mol $dm^{-3}$ $K_4Fe(CN)_6$ + 10 µmol $dm^{-3}$ KCN at the constant potential of 0.6 V

**Fig. 6** Fitting to the detailed photoelectron spectra recorded for steel samples pre-treated for 450 s in 0.1 mol dm$^{-3}$ K$_4$Fe(CN)$_6$ + 10 μmol dm$^{-3}$ KCN at 0.6 V (**a–d**) and in 0.1 mol dm$^{-3}$ K$_4$Fe(CN)$_6$ without KCN (**e–g**). Spectra are presented after subtraction of the Shirley background
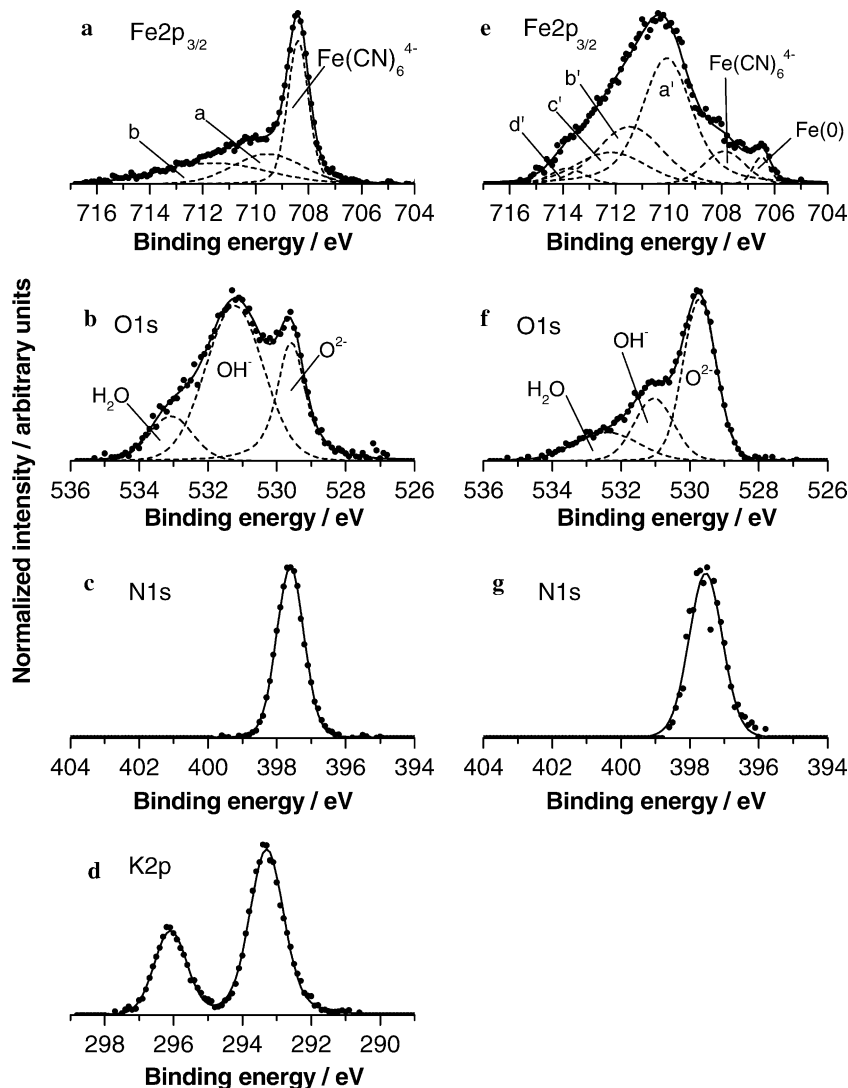


(Fig. 6e) seems to be more complex and may reflect more components than that obtained from the sample conditioned in CN$^-$ containing solution. The peak, marked a' in Fig. 6e, at $E_b = 710.1$ eV is dominating and, most likely, it originates from Fe(II) ions in the oxide/hydroxide passive layer on carbon steel [35–37]. The signal from –Fe$^{II}$(CN)$_6$ groups at $E_b = 707.9$ eV is much less intense and suggests a very small content of PB on the carbon steel surface. This observation is consistent with the results of cyclic voltammetric measurements showing that the surface coverage by PB is less than one monolayer. Other signals shown in Fig. 6e are most likely related to: Fe(0)—metallic iron ($E_b = 706.5$ eV) [35, 39]; b' ($E_b = 711.5$ eV) and c' ($E_b = 712.1$ eV) to iron(III) ions in different compounds constituting the passive layer [35–40]; and d' ($E_b = 713.8$ eV) to the signal of Fe(II) satellite line [37]. It should be emphasized that, in the case of the Fe2p$_{3/2}$ signal (Fig. 6e), the spectrum deconvolution is ambiguous.

More information on the carbon steel surface state upon conditioning in the cyanide-free and cyanide-con-taining potassium hexacyanoferrate(II) solutions can be extracteed from the comparison of XPS O1s signals which are shown in Fig. 6b and f. In general, O1s spectra consist of three signals coming from O$^{2-}$ and OH$^-$ as well as from the oxygen, originating from H$_2$O. All these species are constituents of the oxide/hydroxide passive films on iron and steels [35–37]. It should be remembered that water might be a structural constituent of PB film as well [22–28]. Ranges of binding energies of O1s signals for O$^{2-}$, OH$^-$ and H$_2$O reported in the literature are 529.5–530.3 eV, 531.5–531.6 eV and 532.2–533.6 eV, respectively [35–37, 40, 41]. The binding energies of O1s signals for the sample pretreated in the presence of CN$^-$ are as follows: O$^{2-}$−529.6 eV, OH$^-$−531.2 eV, H$_2$O−533.1 eV; and for the sample pretreated in the cyanide-free K$_4$Fe(CN)$_6$ solution: O$^{2-}$−529.7 eV, OH$^-$−531.0 eV, H$_2$O−532.4 eV. The $E_b$ values determined are in good agreement with literature data. It is noteworthy that the presence of cyanide ions in the pretreatment solution strongly influences the content of oxo-species on the surface of carbon steel samples. For the carbon steel sample conditioned in the

cyanide-containing solution, the content of $OH^-$ ions is higher than that of $O^{2-}$ ions. On the contrary, for the sample pretreated in cyanide-free $K_4Fe(CN)_6$ solution, the content of $O^{2-}$ ions has occurred to be much higher than that of $OH^-$ ions. Since the PB coverage is less than one mololayer in the latter case, the steel surface consists mostly of the iron oxide layer. It can be hypothesized that $CN^-$ ions induce dissolution of iron hydroxide species from the passive layer, and they promote formation of PB film.

X-ray photoelectron spectroscopy signals of nitrogen (N1s) atoms, presented in Fig. 6c and g, are similar to each other, and they are independent of the presence of $CN^-$ ions during the sample pretreatment. The respective binding energies are 397.6 eV and 397.5 eV. The values are close to the binding energies of N1s in $K_4Fe(CN)_6$ ($E_b = 398.0$ eV) and $K_3Fe(CN)_6$

$(E_b = 398.0$ eV) [42] which supports the view that N1s signals originate from $-Fe(CN)_6$ groups in PB. In the case of the sample subjected to the cyanide-containing solution, a well defined XPS signal originating from potassium ions (that are present in PB structure) has been observed. The binding energies are equal to 296.1 eV and 293.3 eV for $K2p_{1/2}$ and $K2p_{3/2}$ peaks, respectively, which are close to the values reported in literature ($K2p_{1/2}$ $E_b = 296.6$ eV and $K2p_{3/2}$ $E_b = 293.9$ eV) [29].

The above mentioned differences in the surface concentrations of elements are even more pronounced during depth profiling (Fig. 7). It is noteworthy, that the oxygen content at the surface is much lower in case of a sample pretreated in the presence of KCN in comparison to the second sample that was not in the contact with the KCN-containing solution. This phenomenon can be explained as follows: the presence of free cyanide ligands in the solution causes dissolution of a native passive (oxide/hydroxide) layer existing on the steel surface. Thus PB film can be better linked to the metal surface. In addition, iron(II) ions arising from the dissolution of hydroxide iron species (from passive layer) can react with hexacyanoferrate(III) ions existing on the sample surface exposed to $K_4Fe(CN)_6$ solution at the potential of 0.6 V versus SCE [at this potential $Fe(CN)_6^{4-}$ ions are oxidized to $Fe(CN)_6^{3-}$] to form PB film.

It is interesting to note that surface concentration of carbon atoms increases after sputtering for 20 min to the value of ca. 3 at.%. The latter value has been observed for the sample conditioned in the cyanide-free solution (Fig. 7). The binding energy of C1s signal for that carbon signal is ca. 283.2 eV which is close to the C1s $E_b$ for iron carbide (283.8 eV) [37]. This result is not surprising provided that the carbon steel contains 2.2 at.% of carbon.

Protective properties of PPy/hcnfe films

To elucidate the influence of the electrodeposition time on the protective properties of the PPy/hcnfe composite film against corrosion, we have recorded potentiodynamic curves (in the solution: 0.1 M HCl + 0.4 M NaCl) for steel samples (Fig. 8): (a) bare steel sample; and the steels covered with the films electrodeposited for (b) 300 s and (c) 900 s, respectively. It is apparent from the data in Fig. 8 that the investigated carbon steel sample does not undergo passivation, and it is characterized by high anodic currents originating from the progress of pitting corrosion of the substrate. Following modification of the steel with a composite polypyrrole based film electrodeposited for 900 s (Fig. 8), the corrosion potential has shifted ca. 100 mV toward more positive values. The most striking feature of the data of Fig. 8 is that the anodic current densities characteristic of steel samples covered with composite films (curves b and c), are almost two orders of magnitude lower when
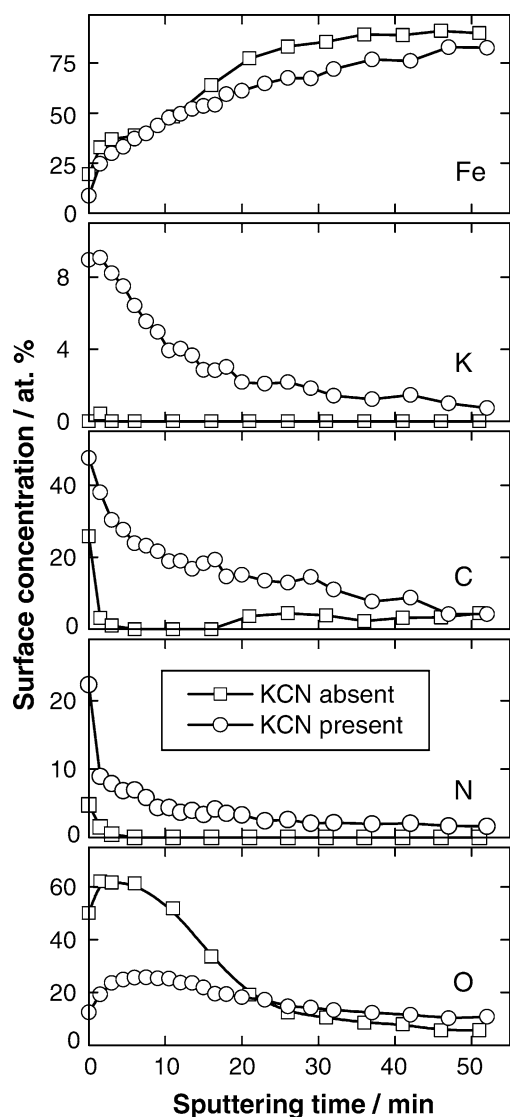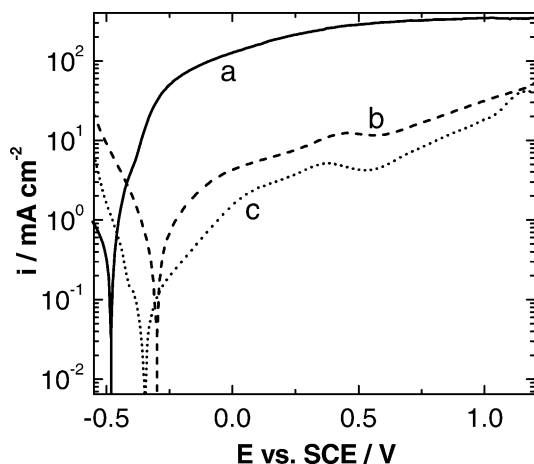
Fig. 7 Depth profiles of the elemental concentrations for steel samples pre-treated as for Fig. 5. A sputtering with $Ar^+$ for 1 min results in etching of a layer of the approximately 1 nm thickness

**Fig. 8** Potentiodynamic curves for **a** bare carbon steel, and for the steels covered with composite films electrodeposited **b** for 300 s and **c** 900 s. Electrolyte 0.1 mol dm$^{-3}$ HCl + 0.4 mol dm$^{-3}$ NaCl. Scan rate 2 mV s$^{-1}$

compared to those characteristic of a bare substrate (curve a). This result is consistent with the strong inhibition of anodic dissolution (pitting corrosion) of electrodeposited composite films.

The process of corrosion in strong acid medium of approximately 0.1 mol dm$^{-3}$ H$^+$ concentration proceeds together with the proton depolarization. The exact nature of the marked increase of the cathodic process occurring at potentials more negative than −0.5 V is unclear. It is difficult to attribute it to the acceleration of hydrogen evolution on PPy/hcnfe film. An alternative explanation may take into account the possibility of discharging or partial reduction of the film components.

The current–time chronoamperometric (potential step) diagnostic measurements were used to determine the resistance of bare and modified steel samples against pitting corrosion in the chloride containing acidic medium. Under such conditions, the uncovered steel sample is subject to rapid pitting corrosion: then the external anodic current exceeds 10$^2$ mA cm$^{-2}$. For the steel sample covered with PPy–HCF film, the measured external currents are at least an order of magnitude lower (Fig. 9).

Figure 9 illustrates chronoamperometric responses recorded for (a) bare steel, and the steels covered with films electrodeposited for (b) 300 s and (c) 900 s, respectively. The film, which has been electrodeposited for shorter period of time (300 s) exhibits moderate protective properties. Consequently, pits have been still formed on a steel substrate but their number and size are significantly (ca. ten times) lower when compared to bare steel. As a result, the external anodic currents observed are more than ten times lower (as apparent from curve b in Fig. 9). Further improvement of the system's protective properties is possible through the increase in the electrodeposition time and, consequently, the increase of the film thickness. It is observed from our experiments that the film electrodeposited for 900 s

possesses the best protective properties. The steel sample covered with such an "optimum" film is characterized by the external anodic current (Fig. 9, curve c) that, during the initial 1–2 min of exposition, rapidly drops and reaches (following 20–30 min) a steady state value on the level of 10$^{-1}$ mA cm$^{-2}$ (inset to Fig. 9). Such low external currents do not lead to the formation of pits. It is likely that, during those initial 1–2 min of exposition, the iron cations originating from the dissolution of steel interacted with Fe(CN)$_6^{3-/4-}$ to form a sparingly soluble interfacial film of PB capable of stabilizing and sealing PPy/hcnfe film. It has been already mentioned that both PB and hexacyanoferrate anions tend to block the access of Cl$^-$ to the steel substrate. A similar phenomenon has previously been observed by us in the case of hexacyanoferrate-containing composite polyaniline-based films on stainless steel [16, 17]. The optimum film was found to protect steel for about 60 h. After that time, pits started to appear as evident from the rising current in the related chronamperometric response [17].

## Conclusions

We have demonstrated the possibility of modification of a carbon steel substrate with a polypyrrole based films containing hexacyanoferrate anions. Such films exhibit promising properties toward the protection of mild steel against pitting corrosion in the chloride-containing acid medium. While having globular morphology, the composite films are fairly dense. Increase in the electrodeposition time from 300 s to 900 s not only produces thicker films but also results in their better stability. It should be stressed that the addition of potassium cyanide (at the concentration level 10 μmol dm$^{-3}$) to the solution used for the preparation of the films dramatically improves the adherence of the PPy/hcnfe coating to carbon steel. Cyclic voltammetric and XPS measurements show that the presence of CN$^-$ ions promotes formation of PB film on carbon steel during its exposure
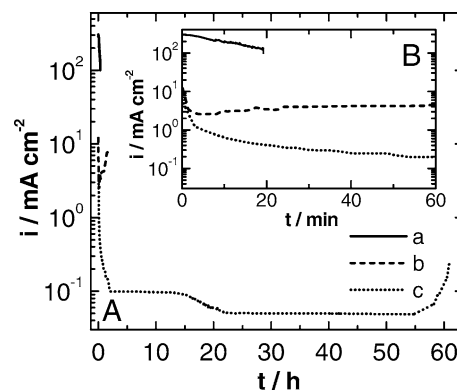


**Fig. 9** Amperometric responses (recorded at 0.5 V) of **a** bare carbon steel, and the steels covered with films electrodeposited for **b** 300 s and **c** 900 s. Electrolyte 0.1 mol dm$^{-3}$ HCl + 0.4 mol dm$^{-3}$ NaCl

to potassium hexacyanoferrate(II) at 0.6 V versus SCE. It is also reasonable to expect that the cyanide ions facilitate the overall adherence of PPy/hcnfe coatings. Finally, due to the presence of immobilized hexacyanoferrate(II,III) anions, the membrane properties of polypyrrole are changed, and the capability of pitting-causing chlorides to undergo sorption [43] in the polymer film is largely suppressed.

# References

1. Milagres BG, de Oliveira Neto G, Kubota LT, Yamanaka H (1997) Anal Chim Acta 347:35
2. Alonso JG, de la Fuente Sanchez C, Garcia MLT, Barbado MDV, Batanero PS (1999) Anal Lett 32:1961
3. Pandey RSS, Takashima W, Kaneto K (2004) J Appl Polym Sci 93:927
4. Raoof JB, Ojani R, Rashid-Nadimi S (2004) Electrochim Acta 49:271
5. Gros P, Durliat H, Comtat M (2000) Electrochim Acta 46:643
6. Desimoni E, Brunetti B, Ugo P, Cazzaniga R (2002) Synth Met 130:135
7. Michalska AJ, Appaih-Kusi C, Heng LY, Walkiewicz S, Hall EAH (2004) Anal Chem 76:2031
8. Michalska AJ, Hall EAH (1999) Electroanalysis 11:756
9. Torres-Gomez G, Skaarup S, West K, Gomez-Romero P (2000) J Electrochem Soc 147:2513
10. Torres-Gomez G, Gomez-Romero P (1998) Synth Met 98:95
11. Malik MA, Wlodarczyk R, Kulesza PJ, Bala H, Miecznikowski K (2005) Corros Sci 47:771
12. Pournaghi-Azar MH, Ojani R (2000) J Solid State Electrochem 4:75
13. Han J, Lee S, Paik W (1992) Bull Korean Chem Soc 13:419
14. Bernard MC, Hugot-Le Goff A, Joiret S, Dinh NN, Toan NN (1999) J Electrochem Soc 146:995
15. Nguyen Thi Le H, Garcia B, Deslouis C, Le Xuan Q (2001) Electrochim Acta 46:4259
16. Kulesza PJ, Miecznikowski K, Malik MA, Gakowski M, Wlodarczyk R, Bala H (2001) Corrosion and corrosion protection, vol 22. The Electrochemical Society, Pennington, p 587
17. Galkowski M, Malik MA, Kulesza PJ, Bala H, Miecznikowski K, Wlodarczyk R, Adamczyk L, Chojak M (2003) J Electrochem Soc 150:B249
18. Tallman DE, Spinks G, Dominis A, Wallace GG (2002) J Solid State Electrochem 6:73
19. Spinks GM, Dominis AJ, Wallace GG, Tallman DE (2002) J Solid State Electrochem 6:85
20. Gros P, Durliat H, Comtat M (2000) Electrochim Acta 46:643
21. Wojda A, Maksymiuk K (1998) J Electroanal Chem 441:205
22. Feldman BJ, Murray RW (1987) Inorg Chem 26:1702
23. Kulesza PJ (1990) J Electroanal Chem 289:103
24. Xidis A, Neff VD (1991) J Electrochem Soc 138:3637
25. Kulesza PJ, Doblhoffer K (1989) J Electroanal Chem 274:95
26. Kulesza PJ, Chelmecki G, Galadyk B (1993) J Electroanal Chem 347:417
27. Kulesza PJ, Zamponi S, Berrettoni M, Marassi R, Malik MA (1995) Electrochim Acta 40:681
28. Zadronecki M, Wrona PK, Galus Z (1999) J Electrochem Soc 146:620
29. Emrich RJ, Traynor L, Gambogi W, Buhks E (1987) J Vac Sci Technol A 5:1307
30. Sauter S, Wittstock G, Szargan R (2001) Phys Chem Chem Phys 3:562
31. Ikeshoji T, Iwasaki T (1988) Inorg Chem 27:1123
32. Engel D, Grabner EW (1988) Zeit Physikal Chem NF 160:151
33. Somani P, Mandale AB, Radhakrishnan S (2000) Acta Mater 48:2859
34. Somani PR, Radhakrishnan S (2002) Mater Chem Phys 77:117
35. Keller P, Strehblow HH (2004) Corros Sci 46:1939
36. Vayer M, Reynaud I, Erre R (2000) J Mater Sci 35:2581
37. Bonnet F, Ropital F, Lecour P, Espinat D, Huiban Y, Gengembre L, Berthier Y, Marcus P (2002) Surf Interface Anal 34:418
38. Suzuki S, Yanagihara K, Hirokawa K (2000) Surf Interface Anal 30:372
39. Wagner CD, Riggs WM, Davis LE, Moulder JF, Muilenberg GE (1979) Handbook of X-ray photoelectron spectroscopy. Perkin–Elmer Corporation
40. Pedraza F, Roman E, Cristobal MJ, Hierro MP, Perez FJ (2002) Thin Solid Films 414:231
41. De Benedetto GE, Guascito MR, Ciriello R, Cataldi TRI (2000) Anal Chim Acta 410:143
42. Buschmann WE, Ensling J, Gutlich P, Miller JS (1999) Chem Eur J 5:3019
43. Inzelt G, Horanyi G (1987) J Electroanal Chem 230:257